SELF-SENSING CONTROL OF PMSM MOTOR FOR WIDE-SPEED RANGE OPERATION

Eisenhawer de M. Fernandes
Department of Mechanical Engineering, Federal University of Campina Grande,
Aprígio Veloso Ave.,882, Campina Grande - Brazil
eisenhawer@ee.ufcg.edu.br

Alexandre C. Oliveira, Antonio M. N. Lima, Cursino B. Jacobina
Department of Electrical Engineering, Federal University of Campina Grande,
Aprígio Veloso Ave.,882, Campina Grande - Brazil
aco@dee.ufcg.edu.br

Welflen R. N. Santos
Federal University of Piauí, Petrônio Portela Ave., Teresina - Brazil
welflen@ufpi.edu.br

Abstract – **This work presents a self-sensing control for permanent-magnet synchronous motor (PMSM) for wide-speed range based on the integration of signal-injection and back-emf tracking methods. It is addressed an evaluation method of the transition region between these approaches based on the harmonic content of the q-axis reference current during self-sensing operation. Based on the procedure, it is established the bandwidth of the rotor position observers in function of the operation speed. It is also addressed the discussion of the attributes of implementation required for integration between the self-sensing techniques. Simulation results are presented showing the performance of the proposed self-sensing wide-speed range system.**

Keywords **- Self-sensing Control, Rotor Position Estimator, Permanent-Magnet Synchronous Motor (PMCM), Wide-Speed Operation.**

I. INTRODUCTION

Permanent-magnet synchronous motor drives (PMSM) has become important competitors to Induction Motor drives (IM) in applications of wide-speed range due to characteristics such as higher efficiency and dynamic performance. PMSM drives require rotor position information which is provided by a rotor position sensor coupled to the motor shaft. The use of rotor position sensor has disadvantages such as increasing cost/volume and reduction of feasibility of drive system [1],[2]. Self-sensing or sensorless solutions have been developed to eliminate the position sensor and estimate rotor position from electrical quantities of the motor, using the motor itself as position sensor.

Self-sensing control methods can be classified in two categories: signal injection methods [1]-[8] and back-emf tracking methods [9]-[14]. Signal injection methods are based on the tracking of the rotor magnetic saliency in the low speed region, exploiting the high-frequency model of the motor when an extra signal is applied. Signal injection methods can be affected by coupling of the fundamental current [5],[13], non-linearities of the voltage converter [6]-[8], and extra power losses [3],[13]. On the other hand, the second category estimates rotor position from the back-emf estimation based on the fundamental model of the machine. The performance of these estimators is dependent on the back-emf amplitude [1] as well as present dynamic stiffness constraints in low speed region [10], [11].

In literature, several solutions that combine signal injection methods (suitable for low speed) and back-emf methods (suitable for high speed) for self-sensing control for wide-speed range has been proposed [8],[14]-[19]. In [8] is proposed a stator flux adaptive observer with Model Reference Adaptative System (MRAS) in which a correction factor, function of the speed, is obtained from the estimation error presented by signal injection technique. In [15], [17] have been proposed the integration between models based on saliency and back-emf estimation in a state filter, the transition between the models is carried out by a non-linear function of the estimated speed. Others solutions are based on hybrid topology that combine rotor flux estimation and signal injection [3],[14], or stator flux estimator and signal injection method [16]. In [18], signal injection technique is combined with a slide-mode observer based on extended back-emf [12] to operate at wide-speed for an Interior Permanent-Magnet Synchronous Motor (IPMSM).

These papers demonstrate the possibility of integration between rotor position estimation techniques with a smooth transition between the responses of the estimators for specific speeds. Usually, the transition rule is a weighting function of the responses, according to the speed. However, there is no discussion about the determination of the transition region between self-sensing techniques in which the rule can be applied.

This work presents a self-sensing control for permanent-magnet synchronous motor for wide-speed range based on the integration of signal-injection method and back-emf tracking method. It is addressed an evaluation method of the transition region between the methods based on the harmonic content of the q-axis reference current during the self-sensing operation. Based on the procedure, it is established the bandwidth of the rotor position observers in function of the operation speed. The work also presents the discussion of the attributes of implementation required for integration between the self-sensing techniques. A complete set of simulation results for wide-speed range is presented.

In Section II is addressed the signal injection method used to estimate rotor position at low speeds. In Section III is presented the method used to estimate rotor position at medium and high speeds, the technique is based on tracking the back-emf of the motor. Section IV presents the structure of the self-sensing control system. In Section V addressed the proposed method for determing the transition region between the rotor estimation methods and how the responses can be combined during the transition region. Besides, it is discussed the way the signal injection method can be initialized or disabled during operation. Section VI presents the conclusions of the work.

II. LOW SPEED OPERATION – SIGNAL INJECTION METHOD

The rotor position estimation methods used at low speeds are based on the detection of saliency orientation of the machine [1]. The saliency estimation is performed by the injection of High-Frequency (HF) voltage excitation with frequency ω_h and magnitude V_h in the stationary reference frame (1).

$$v_{sdqh}^s = V_h e^{j\omega_h t} \tag{1}$$

The resulting high-frequency current (2) has two components: a positive-sequence and a negative-sequence. The rotor position information is presented in the negative sequence component ($2\theta_r$).The machine saliency modulates the HF current amplitude.

$$i_{sdqh}^s = I_{hp} e^{j\omega_h t} + I_{hn} e^{j(-\omega_h t + 2\theta_r)} \tag{2}$$

Where:

$$I_{hp} = -\left(jV_h/2\omega_h l_{sd} l_{sq}\right)\left(l_{sd} + l_{sq}\right) \tag{3}$$

$$I_{hn} = \left(jV_h/2\omega_h l_{sd} l_{sq}\right)\left(l_{sd} - l_{sq}\right) \tag{4}$$

I_{hp} is the amplitude of the positive-sequence of HF current component, I_{hn} is the amplitude of the negative-sequence of HF current component, l_{sd} is the d-axis inductance, l_{sq} is the q-axis inductance of the motor, θ_r is the rotor position, j is the complex operator.

Several techniques to extract the position information are proposed in the literature [1]-[7]. In Fig. 1 is shown a demodulation scheme composed by a Band-Pass Filters (BPF) and Synchronous-Frame Filtering [5],[7]. The remaining signals $p_{\alpha\beta}$ contain the rotor position information ($2\theta_r$). These signals can be expressed by (5).

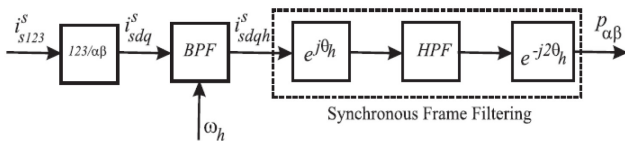$$p_{\alpha\beta} = I_{hn} e^{j2\theta_r t} \tag{5}$$

Fig. 1. Demodulation scheme for rotating voltage injection.

The position signals $p_{\alpha\beta}$ are applied to the input of Luenberger-style observer [11]. The rotor position estimator is composed by heterodyning process, a controller (k_{i_sal}, k_{o_sal}, b_{o_sal}) and the physical model of the motor. The observer provides the estimated mechanical rotor position ($\hat{\theta}_{rm\_sal}$) and speed ($\hat{\omega}_{rm\_sal}$), see Fig. 2. This rotor position estimator has property of zero lag estimation due to reference torque feedforward T_e^*[11].
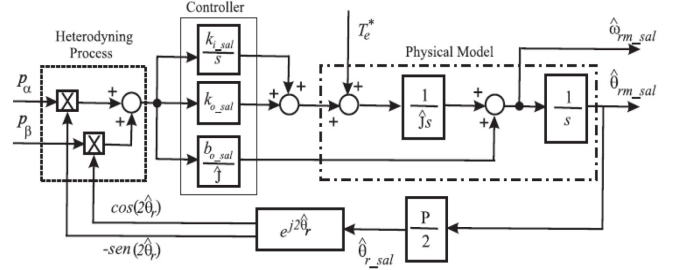

Fig.2. Saliency-tracking observer at low speed.

III. HIGH SPEED OPERATION – BACK-EMF ESTIMATION

For PMSM motor operation at medium and high speeds is required the use of estimation methods based on back-emf tracking. The information of the rotor position is extracted from back-emf estimation, thus, it is not necessary the application of extra signal. In this work, it has implemented the method proposed by [11]. The technique employs two cascaded estimators, one for back-emf estimation and other for rotor position estimation.

The back-emf estimator is a current state-filter implemented in the stationary reference-frame, the structure is illustrated in Fig. 3. The structure is based on the extended back-emf model proposed by [12]. The estimated back-emf has the rotor information and the estimation error is applied to the input of the rotor position observer (Fig. 4). The rotor position observer is a Luenberger observer which its output is the estimated mechanical speed ($\hat{\omega}_{rm\_bemf}$) and rotor position ($\hat{\theta}_{rm\_bemf}$).
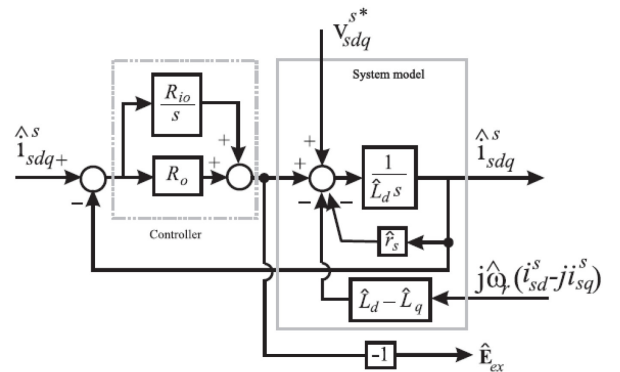

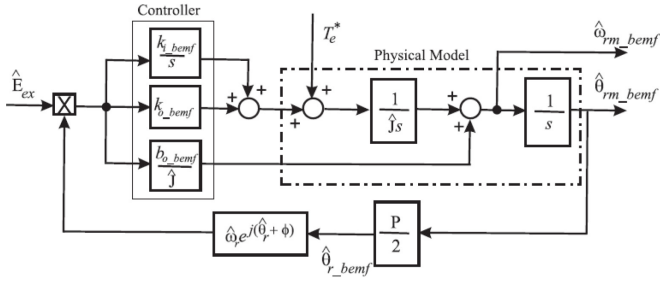Fig.3. State-filter for stationary current and back-emf estimation.

Fig.4. Back-emf tracking observer at high speed operation.

IV. SELF-SENSING CONTROL SYSTEM

The self-sensing speed control system for wide-speed range is illustrated in Fig. 3. The system has been implemented in the software PSIM/C++. The speed controller is composed by a PI regulator with bandwidth set at 10 Hz. The bandwidth of the speed controller has been chosen in order to have the poles of the speed closed loop transfer function real and identical. Then, the proportional and integral gains of the speed controller provide a bandwidth of 10 Hz.

The current controller is a PI regulator with cross-coupling decoupling term and compensation of back-emf. The reference current of d-axis i_{sd}^{r*} is set to zero. The reference i_{sq}^{r*} current is defined by the output of the torque vector control block. The bandwidths of the current controllers are identical and set to 250 Hz. The gains of the current controllers have been chosen based on the pole placement approach in order to cancel the pole of the electrical system.

The high-frequency voltage has specification of 60 V-1,0 kHz. The sampling frequency f_s of the variables is 100 μs. The DC-link voltage E_d is 300 V. The block 'Rotor Position Estimators for Wide-speed' is composed by the saliency-tracking observer, back-emf tracking observer, the rule of the adjustment of observers' bandwidths (block 'Specification of BWO') and the Transition Function between the self-sensing strategies.

The bandwidth of each observer has been set using the pole placement approach. The PMSM motor has the following rated parameters: r_s= 6,2 Ω, l_{sd}= 24 mH, l_{sq}= 33 mH, back-emf constant= 56,16 V/krpm, J= 0,084.10⁻³ kg.m², I_N= 2,0 A, V_N= 200 V (phase-to-phase), P= 400 W and speed = 3000 rpm (400 Hz).
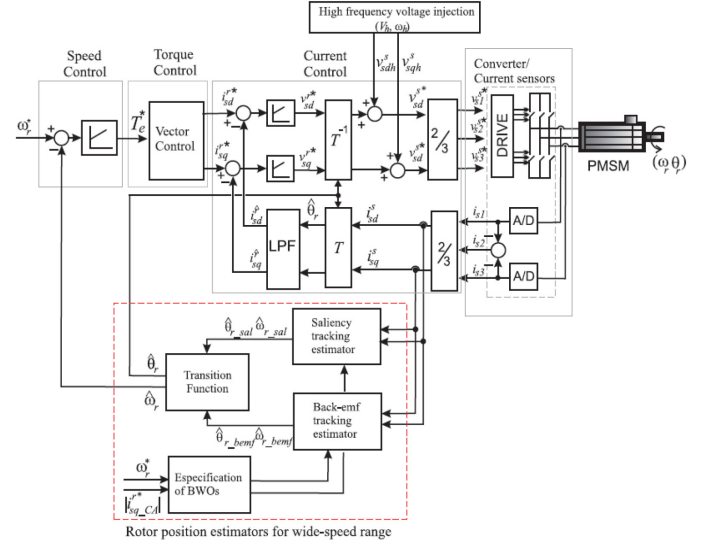

Fig.5. Diagram of the self-sensing speed control system speed for whole speed range.

V. TRANSITION REGION BETWEEN THE TECHNIQUES

This section presents the methodology to combine the responses provided by the rotor position observers. In literature, there is no discussion or little information about a criterion to changeover between the techniques. Thus, is proposed a procedure to determine the transition region between the each observer using as metric the harmonic content of the reference current i_{sq}^{r*} ($\left|i_{sq\_AC}^{r*}\right|$) allowing to integrate the rotor position observer in order to compose a rotor position estimator for whole speed operation.

The transition region can be obtained from the evaluation of the profile of the calculated rms AC content [19] of reference current i_{sq}^{r*} varying the bandwidth of each position observer (BWO) in function of the operation speed (ω_r). The procedure to determine the transition region has the following steps:

1. Evaluate the profile of the estimated speeds in function of the operating speed, varying the observer's bandwidths;

2. Obtain the harmonic content profile of the reference current $i_{sq\_CA}^{r*}$ in function of the speed ω_r for different values of observer's bandwidth;

3. Superposition of the $i_{sq\_AC}^{r*}$ profiles of each observer versus rotor speed in function of the observer's bandwidth;

4. Determination of the admissible threshold value for harmonic content level $\left|i_{sq\_AC}^{r*}\right|$ of for whole speed and be identical for both estimation techniques;

4. The transition region which both estimation techniques present acceptable performance can be identified by the superposition of the curves and the level $\left|i_{sq\_AC\_MAX}^{r*}\right|$;

5. Set the tuning of the position observers that fulfill condition 4 in the transition region;

6. Determine the combination between the observers' responses and the contribution of each response.

In this work, the combination between the observers' responses ($\hat{\theta}_{rm\_BLND}$) is given by:

$$\hat{\theta}_{rm\_BLND} = \alpha\hat{\theta}_{rm\_sal} + (1-\alpha)\hat{\theta}_{rm\_bemf} \qquad (6)$$

where α is a parameter that set the contribution of each estimator in the transition region. The choice of this parameter is addressed in the subsection *C*.

A. Determination of the transition region

Based on the procedure aforementioned, each rotor position estimation technique has been evaluated. The results are shown in Fig.6 emphasizing the profile of the harmonic content presented in the reference current i_{sq}^{r*} ($\left| i_{sq\_AC}^{r*} \right|$) varying the reference speed and observer bandwidth. As can be seen, when rms AC content $\left| i_{sq\_AC}^{r*} \right|$ is greater than 4% of the rated current I_N occurs a fast increasing of this quantity.

A rapid variation of $\left| i_{sq\_AC}^{r*} \right|$ can lead to faults such as excessive heating or improperly action of the protection system [22]. Thus, it has established as admissible threshold for $\left| i_{sq\_AC}^{r*} \right|$ that $\left| i_{sq\_AC}^{r*} \right| < 0,04I_N$ for whole speed region. In this manner, the intersection between the $\left| i_{sq\_AC}^{r*} \right|$ curves for both techniques satisfying this criterion is the transition region between the self-sensing strategies. For the system in study, the transition region is the speed range from 20 Hz or (125 rad/s) to 30 Hz (188 rad/s).
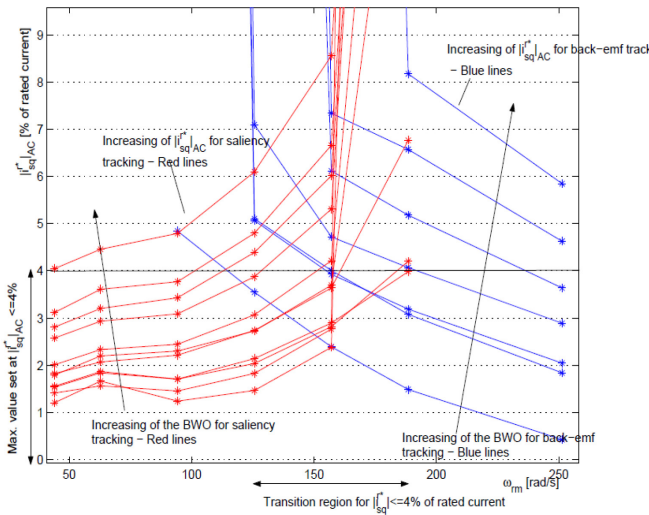

Fig.6. Transition region between rotor estimation techniques assuming $\left| i_{sq\_AC}^{r*} \right| < 0,04I_N$: saliency-tracking method (red), back-emf estimation (blue).

B. Bandwidth of the rotor position observers

The tuning of the rotor position observers was defined according to the criterion that $\left| i_{sq\_AC}^{r*} \right| < 0,04I_N$. In Fig. 7 is

shown the bandwidth curve of the saliency-tracking observer (red) and bandwidth of the back-emf observer (blue). The tuning of the observers gains is dependent on the rotor speed ω_r . For the back-emf observer, one can verify that reducing of the speed should be followed with the reduction of the observer's bandwidth [10]. In similar manner, when the control system operates at low speed and is demanded to increase the rotor speed, the saliency-tracking observer's bandwidth should be reduced.
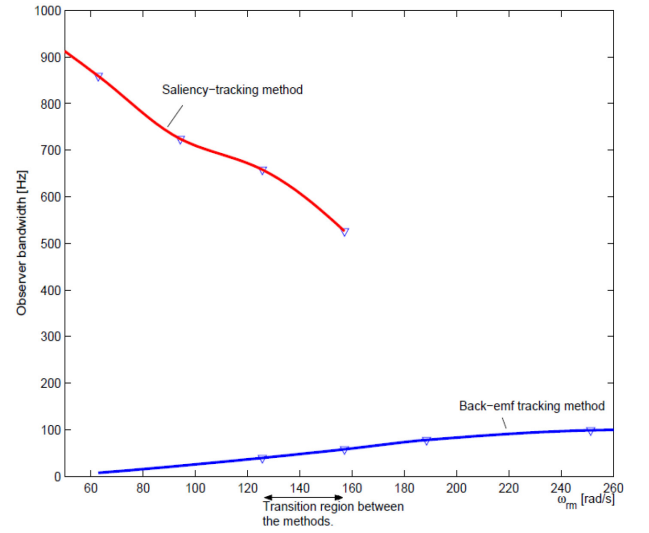

Fig.7. Observers' bandwidths assuming $\left| i_{sq\_AC}^{r*} \right| < 0,04I_N$: saliency-tracking method (red), back-emf estimation (blue).

C. Selection of the parameter α

The contribution of each observer response in the transition region is represented by the parameter α (6). One important feature is how to set this parameter related to the speed. Different relations have been proposed in literature for this parameter, linear [15], [18] or non-linear functions [16]. In this work, it has been established that the profile of α is a linear function of ω_r such that if $\omega_r < \omega_{r\_low}, \alpha = 1$, and if $\omega_r > \omega_{r\_high}, \alpha = 0$.

D. Self-sensing speed control

Simulation results for self-sensing speed control system shown in Fig. 5 are presented in this section. It has been tested two operation conditions: speed ramp command and speed reversal. In Fig. 8 is shown the results for speed ramp command from 0 Hz to 60 Hz during 10s. After the speed reference is constant and decreased to zero at t=25s. The tuning of the rotor position estimators (saliency-tracking and back-emf tracking) occurs as function of the reference speed in order to present the bandwidth shown in Fig.7 and maintain the harmonic content of i_{sq}^{r*} below $0,04I_N$.
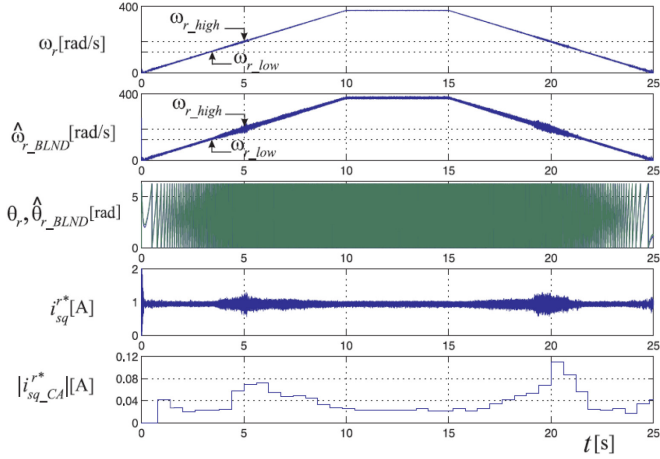
Fig.8. Self-sensing control for reference speed in ramp (0Hz- 60 Hz): rotor speeds (ω_r, $\hat{\omega}_{r\_BLND}$), rotor positions (θ_r, $\hat{\theta}_{r\_BLND}$), reference current (i_{sq}^{r*}) and rms AC content $\left|i_{sq\_AC}^{r*}\right|$.

In Fig. 8 is shown the measured and estimated speeds (ω_r, $\hat{\omega}_{r\_BLND}$) rotor positions (θ_r, $\hat{\theta}_{r\_BLND}$), reference current i_{sq}^{r*} and the rms AC content of i_{sq}^{r*} $\left|i_{sq\_AC}^{r*}\right|$. The rms AC value of i_{sq}^{r*} is performed by FFT (Fast Fourier Transform) of the waveform based on a window with 1024 samples. The transition region between the estimation techniques is represented by the symbols ω_{r_low} and ω_{r_high}. As can be seen, it is verified good performance under self-sensing control with the harmonic content of i_{sq}^{r*} below specified limit ($0{,}04I_N$).

In Fig. 9 is shown the results for self-sensing control under speed reversal from -377 rad/s (-60 Hz) to $+377$ rad/s (60 Hz). It is presented the measured and estimated speeds (ω_r, $\hat{\omega}_{r\_BLND}$), rotor positions (θ_r, $\hat{\theta}_{r\_BLND}$), reference current i_{sq}^{r*} and the rms AC content of i_{sq}^{r*} $\left|i_{sq\_AC}^{r*}\right|$ Besides, it is emphasized the rotor position waveforms θ_r, $\hat{\theta}_{r\_BLND}$.

In Fig. 10 is presented the same operation condition showing the instants of enabling/disabling of the high-frequency signal injection (*HF on/HF off*). The signal injection method is applied until the motor speed be greater than ω_{r_high} during the ramp, after this, is zero. The voltage is applied again when $\omega_r < 1{,}05\omega_{r\_high}$. In simulations the load torque applied is 25% of the rated torque.
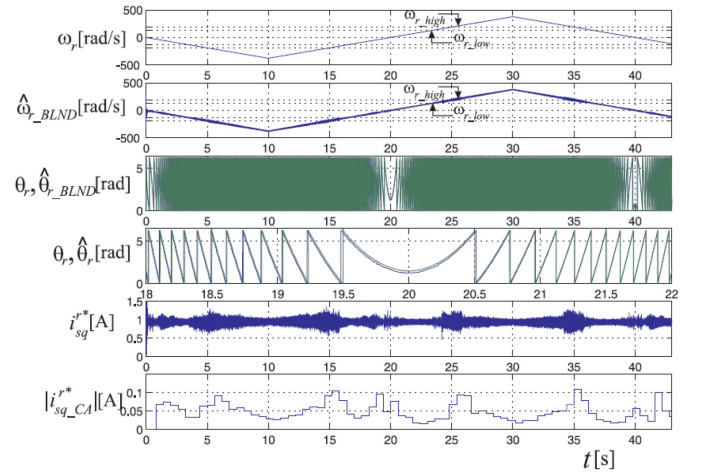

Fig.9. Self-sensing control for speed reversal (-60Hz- 60 Hz): rotor speeds (ω_r, $\hat{\omega}_{r\_BLND}$), rotor positions (θ_r, $\hat{\theta}_{r\_BLND}$), reference current (i_{sq}^{r*}) and rms AC content $\left|i_{sq\_AC}^{r*}\right|$.
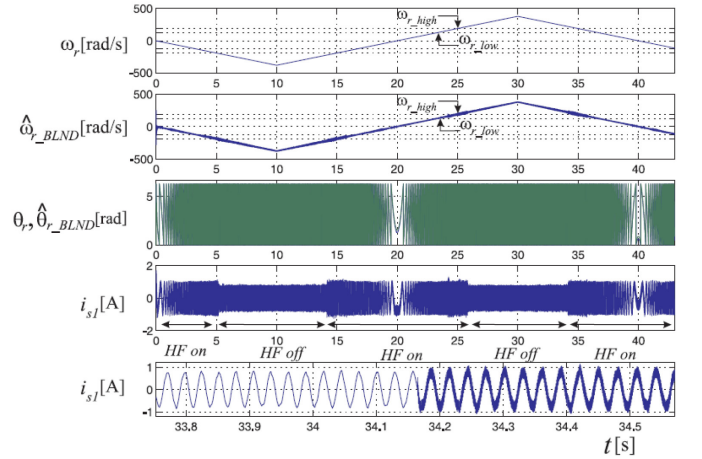

Fig.10. Self-sensing control for speed reversal (-60Hz- 60 Hz): rotor speeds (ω_r, $\hat{\omega}_{r\_BLND}$), rotor positions (θ_r, $\hat{\theta}_{r\_BLND}$), phase current i_{s1}.

E. Initialization of the signal injection method

One important issue according to integration of the self-sensing methods is the initialization of saliency-tracking observer. After the disabling of signal injection, the saliency-tracking estimator should be initialized with current values of back-emf estimator, i.e., $\hat{\omega}_{r\_sal}(k-1) \leftarrow \hat{\omega}_{r\_bemf}(k)$ and $\hat{\theta}_{r\_sal}(k-1) \leftarrow \hat{\theta}_{r\_bemf}(k)$. Otherwise, if the saliency-tracking observer is arbitrarily initialized, $\hat{\omega}_{r\_sal}(k-1) \neq \hat{\omega}_{r\_bemf}(k)$ and $\hat{\theta}_{r\_sal}(k-1) \neq \hat{\theta}_{r\_bemf}(k)$ the observer could converge to different values of real speed and position. This behavior of the saliency-tracking observer is shown in Fig. 11 for different initialization conditions.
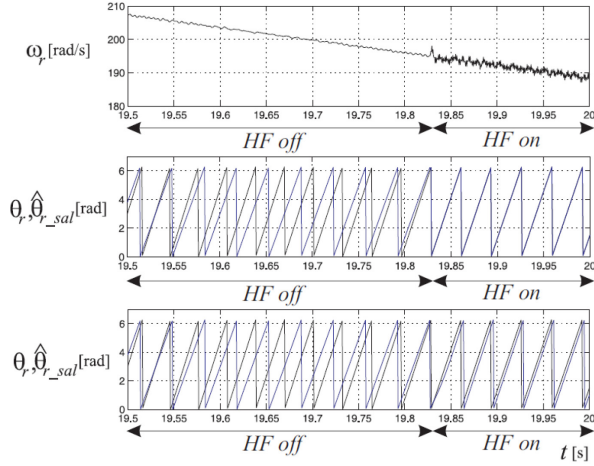
Fig.11. Initialization of the saliency-tracking observer (top to bottom): measured speed, rotor positions when

$$\hat{\omega}_{r\_sal}(k-1) \leftarrow \hat{\omega}_{r\_bemf}(k), \hat{\theta}_{r\_sal}(k-1) \leftarrow \hat{\theta}_{r\_bemf}(k), \text{ rotor}$$

positions with arbitrary initialization

$$\hat{\omega}_{r\_sal}(k-1) \neq \hat{\omega}_{r\_bemf}(k), \hat{\theta}_{r\_sal}(k-1) \neq \hat{\theta}_{r\_bemf}(k).$$

VI. CONCLUSION

The paper has presented an evaluation of the performance of self-sensing control of PM motor for wide-speed range. The self-sensing control is based on the combination of signal-injection method, suitable for low speeds and a back-emf tracking method used for medium and high speeds. It has addressed a procedure for determining the transition region between rotor position estimator techniques allowing for the integration of the responses.

The integration between the rotor position observers is based on the evaluation of the harmonic content of the commanded current and estimated speed provided by each observer. The self-sensing control for wide-speed operation has been implemented in software (C++/PSIM) and simulation results are presented demonstrating the performance of the control system.

ACKNOWLEDGEMENT

REFERENCES

[1] J.-H. Jang, J.-I. Ha, M. Ohto, K. Ide, S.-K. Sul, "Analysis of permanent-magnet machine for sensorless control based on high frequency signal injection", *IEEE Transactions on Industry Applications*, vol. 39, no. 6, pp.1595-2004, May/June 2003.

[2] M. J. Corley, R. D. Lorenz, "Rotor Position, Velocity Estimation for a Salient-pole Permanent Magnet Synchronous Machine at Standstill and High Speed", *IEEE Trans. on Industry Applications*, vol. 34, no. 4, pp. 784-789, July/August 1998

[3] G.D. Andreescu, C. I. Pitic, F. Blaabjerg , I. Boldea, "Combined flux observer with signal injection enhancement for wide speed range sensorless direct torque control of IPMSM drives", *IEEE Transactions on Energy Conversion*, vol.23, no. 2 , pp. 393-401, June 2008.

[4] J. Holtz, "Acquisition of position error and magnet polarity for sensorless control of PM Synchronous Machines", *IEEE Transactions on Industry Applications*, vol. 44, no. 4, pp. 1172-1180, July/August 2008.

[5] C. Caruana, G. M. Asher, M Sumner, "Performance of HF Signal Injection Techniques for Zero-Low-Frequency Vector Control of Induction Machines Under Sensorless Conditions", *IEEE Transactions on Industrial Electronics*, vol. 53, no.1, pp. 225-238, February 2006

[6] J. M. Guerrero, M. Leetmaa, F. Briz, A. Zamarrón, R. D. Lorenz, "Inverter Nonlinearity Effects in High-Frequency Signal-Injection-Based Sensorless Control Methods", *IEEE Transactions on Industry Applications*, vol. 41, no. 2, pp. 618-626, March/April 2005.

[7] E. M. Fernandes, A. C. Oliveira, A. M. N. Lima, C. B. Jacobina, "Estimação de posição rotórica de motor pmsm com minimização da distorção da tensão de alta frequência", *Brazilian Journal of Power Electronics*, vol. 17, no. 1, pp. 447-455, February/April 2012.

[8] A. Piippo, J. Solamaki, J. Luomi, "Signal injection in sensorless PMSM drives equipped with inverter output filter", *IEEE Transactions on Industry Applications*, vol. 44, no. 5, pp. 1614-1620, October 2008.

[9] L. A. S. Ribeiro, M. C. Harke, R. D. Lorenz, "Dynamic properties of back-emf based sensorless drives", *in Proc. of IAS*, vol. 4, pp. 2026-2033, October 2006.

[10] R. W. Hejny, R. D. Lorenz, "Evaluating the practical low speed limits for back-emf tracking-based sensorless speed control using drive stiffness as a key metric", vol. 4, *in Proc. of ECCE*, pp. 2481-2488, September 2009.

[11] H. Kim, *On-line Parameter Estimation, Current Regulation, and Self-sensing for IPM Synchronous Machine Drives*, University of Wisconsin-Madison, USA, 2004.

[12] S. Morimoto, K. Kawamoto, M. Sanada, Y. Takeda, "Sensorless control strategy for salient-pole PMSM based on extended EMF in rotating reference frame", *IEEE Transactions on Industry Applications*, vol. 38, no. 4, pp. 1054-1061, July/August 2002.

[13] S. Ovrebo, *Sensorless Control of Permanent Magnet Synchronous Machine,* Norwegian University of Science and Technology (NTNU), 2004.

[14] C. Silva, G. M. Asher, M. Sumner, "Hybrid rotor position observer for wide speed-range sensorless PM motor drives including zero speed", *IEEE Transactions on Industrial Electronics*, vol. 53, no. 2, pp. 373-378, April 2006.

[15] T. Frenzke, B. Piepenbrier, "Position-sensorless control of direct drive permanent magnet synchronous motors for railway traction", *in Proc. of PESC*, pp. 1372-1377, June 2004.

[16] G. Foo, S. Sayeef, M. Rahman, "Low-speed and standsitll operation of a sensorless direct torque and flux controlled IPM synchronous motor drive", *IEEE Transactions on Energy Conversion*, pp.25-33, vol. 25, no.1, March 2010.

[17] M. Schroedl, M. Hoffer, W. Staffler, "Sensorless control of PM synchronous motors in the whole speed range including standstill using a combined inform/emf model", *in Proc. of EPE-PEMC*, pp. 1943- 1949 2006.

[18] G. Wang, R Yang, D. Xu, "DSP-based Control of Sensorless of IPMSM Drives for Wide-Speed Range Operation", *IEEE Transactions on Industrial Electronics*, vol. 60, no. 2, pp. 720-727, February 2013.

[19] H. Akagi, E. H. Watanabe, M. Aredes, *Instantaneous Power Theory and Applications to Power Conditioning*, John Wiley & Sons, 2007.